Food Chemistry 210 (2016) 520–529

Contents lists available at ScienceDirect

Food Chemistry

journal homepage: www.elsevier.com/locate/foodchem

Comparative characterization of the deamidation of carboxylic acid deamidated wheat gluten by altering the processing conditions

Lan Liao *, Xueyue Han, Lin-ping Chen, Li Ni, Zhi-bin Liu, Wen Zhang, Qing Chen

Institute of Food Science and Technology, College of Biological Science and Technology, Fuzhou University, Fuzhou, Fujian 350108, People's Republic of China
Fujian Center of Excellence for Food Biotechnology, Fuzhou University, Fuzhou, Fujian 350108, People's Republic of China

ARTICLE INFO

Article history:
Received 9 January 2016
Received in revised form 23 April 2016
Accepted 25 April 2016
Available online 26 April 2016

Keywords:
Wheat gluten
Deamidation
Aggregation
Functional properties
Structure
Processing conditions

ABSTRACT

The physicochemical, structural and functional properties of citric-acid-deamidated wheat gluten at controlled degrees of deamidation (25%, 40% and 55%), which were obtained by using different acid concentrations (3.93×10^{-5}, 3.14×10^{-3} and 2.36×10^{-2} mol/L) and temperatures (70 °C 2 h, 90 °C 1 h and 110 °C 40 min), were compared. Various deamidation processing conditions leading to the same degree of deamidation resulted in proteins with different physicochemical and structural characteristics, as indicted by the degree of hydrolysis, Z-potential, surface hydrophobicity, particle size, SDS-PAGE results, SEC-HPLC results, intrinsic fluorescence and FTIR spectra. Agglomerative hierarchical clustering analysis and principal component analysis qualitatively indicated a significant effect of pH on protein deamidation. Three samples at 40% deamidation, which were produced by a moderate acid concentration, showed the best emulsifying and foaming properties. Processes conducted at greater than 90 °C causing protein aggregation and at a high acid concentration rupturing peptide bonds, impaired protein quality. These findings demonstrated that a limited amount of H^+ could function well in the catalysis of the deamidation of amide groups without an excess of H^+, which hydrolyses peptide bonds in a stronger hydrothermal treatment.

1. Introduction

Wheat gluten is useful in the food industry, but its application is limited because of its water-insolubility. The solubility of wheat gluten can be improved by deamidation via heating in acid. Glutamine and asparagine residues are transformed into carboxyl groups via the formation of hydrogen bonds, and heating in acid increases the hydrophobic interactions and electrostatic repulsion of the protein molecular chains. This processing causes protein dissociation, increasing the solubility of the protein (Zhao, Tian, & Chen, 2011). It has been reported that deamidation by heating in acid improved the functional properties of wheat proteins and produced a modified wheat gluten with a lower immunoreactivity to celiac IgA antigliadin antibodies and reduced its cytotoxic activity in a human colon adenocarcinoma LoVo cell line (Berti et al., 2007; Du et al., 2009; Liao et al., 2010a, 2010b; Webb, Naeem, & Schmidt, 2002).

Recent investigations have revealed that carboxylic acid deamidation via hydrothermal treatment modified proteins to have desirable functions, but had little effect on the hydrolysis of protein bonds. A hydrothermal treatment is necessary to deamidate proteins. For a protein used as an emulsifying and foaming agent, the retention of large molecular constituents is crucial (Wong, Choi, Phillips, & Ma, 2009). Deamidation under extremely acidic conditions leads to the excessive breakage of peptide bonds, destroying certain protein functions. Deamidation of proteins that contain carboxylic acids via heating has been considered to be an effective method to minimize peptide bond hydrolysis and enhance the functional properties and safety of wheat proteins (Liao et al., 2010a, 2010c). After this type of modification, wheat gluten protein molecules become flexible, exhibit desirable changes in their protein structure and have better functional properties (Liao, Liu, Zhao, Zhao, & Cui, 2011), and essential amino acids in wheat gluten and gluten are preserved (Lei, Zhao, Selomulya, & Xiong, 2015), significantly improving the emulsifying and foaming properties of gliadin (Qiu, Sun, Zhao, Cui, & Zhao, 2013). Matsudomi, Sasaki, Tanaka, Kobayashi, and Kato (1985) reported that hydrophobic interactions and the formation disulphide bonds due to the hydrothermal treatment of ovalbumin aggregates led to desirable functional properties. Heat treatment increases the degree of protein aggregation by forming interchain disulphide bonds (Wagner, Morel, Bonicel, & Cuq, 2011), which involves sulfhydryl and disulphide interchange reactions, which fix the protein in a denaturated state (Morel, Redl, & Guilbert, 2002). Liao et al.

* Corresponding author at: Institute of Food Science and Technology, Fuzhou University, Xue Yuan Road, University Town, Fuzhou, People's Republic of China.
E-mail address: felliao@fzu.edu.cn (L. Liao).

http://dx.doi.org/10.1016/j.foodchem.2016.04.113
0308-8146/

demonstrated that the slight breakage of peptide bonds (<1%) in wheat gluten aggregates during deamidation by heating in acid achieved a balance between the successive opening-up of the network structure by electrostatic repulsion and the thermal cross-linking of sulfhydryls (Liao et al., 2011).

It is well recognized that the deamidation conditions play a significant role in the conformational and functional properties of a protein. Different processing conditions, for example, varying the temperature or pH, may produce modified proteins with similar functional properties. However, attempts which have been extensively performed on the functional and structural characterization of proteins after acid deamidation, has usually been restricted to a single processing condition. To date, few reports are available concerning detailed scientific comparisons of wheat gluten proteins that have similar degrees of deamidation produced by different deamidation processing conditions, such as different temperatures and acid concentrations (pHs). Therefore, our approach was to directly produce wheat gluten with three different degrees of deamidation (~25%, ~40% and ~55%) based on screening trials with different heating conditions and acid concentrations. We compared the aggregation state of the deamidated wheat gluten proteins with specific degrees of deamidation. Changes in the functional and conformational properties of the wheat glutens proteins were also determined to investigate their properties at the same degree of deamidation resulting from different processing conditions. We finally discuss our results by applying pattern recognition techniques based on an agglomerative hierarchical clustering (AHC) analysis and principal component analysis (PCA) to compare the behaviour of deamidated wheat gluten proteins.

2. Materials and methods

2.1. Materials, chemicals and reagents

A wheat gluten isolate was first prepared by hand washing a dough-ball with excess distilled water from the strong wheat cultivar Zhoumai 22 (supplied by a wheat farmer from the Henan province of China) after extracting the lipids with chloroform. The freeze-dried wheat gluten was ground in a coffee grinder. The protein (N × 5.7 g/kg), carbohydrate and moisture contents were analysed using AOAC methods (Redondo-Cuenca, Villanueva-Suarez, & Mateos-Aparicio, 2008) and were 845.4 ± 70.3 g/kg, 68.8 ± 1.0 g/kg and 85.8 ± 1.3 g/kg, respectively. All other chemicals and solvents were of analytical or HPLC grade and obtained from the Sinopharm Chemical Reagent Co. Ltd. (Shanghai, China) and Sigma Chemical Co. Ltd. (St. Louis, USA), respectively.

2.2. Deamidation of wheat gluten with citric acid

The deamidation of wheat gluten via different hydrothermal treatments at different citric acid concentrations was conducted according to our previously published method (Liao et al., 2011) based on screening trials (Fig. 1 and Table 1). Briefly, wheat gluten (50 g/L) was mixed with different citric acid (3.93×10^{-5}, 3.14×10^{-3} and 2.36×10^{-2} mol/L) solutions to form suspensions. Subsequently, the suspension with a citric acid concentration of 3.93×10^{-5} mol/L was divided into three aliquots. The aliquots were hydrated for 120 min in a shaking water bath at room temperature and heated at 70 °C for 2 h (**I**), 90 °C for 1 h (II) and 110 °C for 40 min (III) in an autoclave and then immediately placed in an ice water bath for 5 min to stop the reaction. The solutions were centrifuged at 10, 000*g* for 10 min at 4 °C and the supernatants (soluble fraction) were collected with a syringe. The supernatants were dialysed in deionized water at 4 °C for 24 h to remove the ammonium ions and were designated as citric acid deamidated wheat gluten (CDWG) at a 25.13 ± 1.5% degree of deamidation (DD) (abbreviated as CDWGI-25, CDWG II-25 and CDWGIII-25, respectively). The suspensions with citric acid concentrations of 3.14×10^{-3} and 2.36×10^{-2} mol/L were submitted to a similar process, producing citric acid deamidated wheat gluten at 40.05 ± 1.5% and 55.15 ± 1.9% DD, respectively (abbreviated as CDWGI-40, CDWG II-40, CDWGIII-40, CDWGI-55, CDWG II-55 and CDWGIII-55).

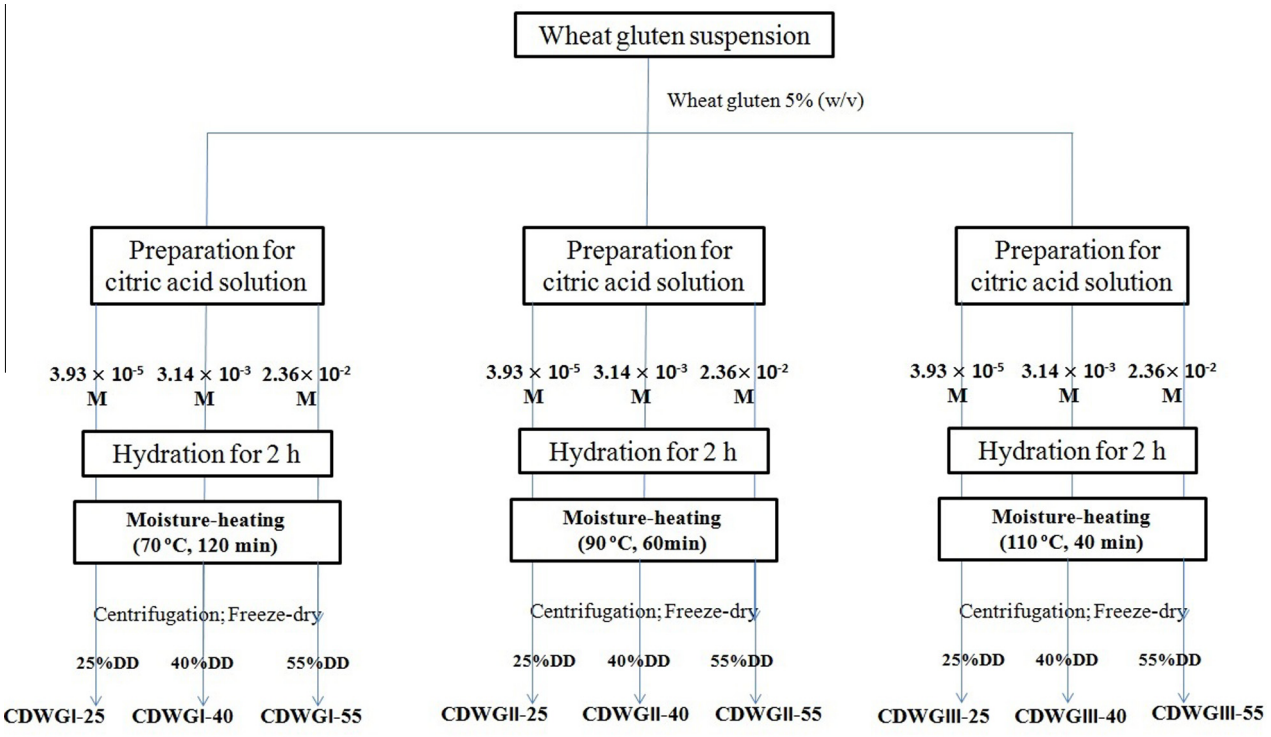

Fig. 1. Process diagram of the deamidated wheat gluten with citric acid at three levels of degree of deamidation obtained by different deamidation processing conditions (70 °C (CDWG-I), 90 °C (CDWG-II) and 110 °C (CDWG-III)).

Table 1
Changes of physicochemical and functional properties of CDWGs at three levels of degree of deamidation obtained by different deamidation processing conditions (70 °C (CDWG-I), 90 °C (CDWG-II) and 110 °C (CDWG-III)).

Temperature (°C)	DD[a] (%)	DH[b] (%)	S_0[c]	Zeta potential (mv)	Particle size (nm)	EAI[d] ($m^2 g^{-1}$)	ESI[e] (min)	Foaming capacity (%)	Foaming stability (%)
70	25	$1.19 \pm 0.24a$	7077.4_b	$3.24 \pm 0.13_a$	$359.25 \pm 1.18_a$	$17.65 \pm 0.59_b$	$31.38 \pm 0.70_b$	$159.09 \pm 6.43_d$	$80.07 \pm 3.23_b$
70	40	$2.64 \pm 0.08_b$	8388.6_d	$22.2 \pm 1.35_b$	$328.10 \pm 0.84_a$	$25.09 \pm 2.89_d$	$65.35 \pm 0.51_c$	$136.36 \pm 2.31_c$	$83.33 \pm 4.71_b$
70	55	$2.74 \pm 0.06_b$	7513.3_c	$20.6 \pm 0.40_b$	$1323.00 \pm 2.82_c$	$22.28 \pm 0.58_c$	$57.61 \pm 1.57_{bc}$	$122.72 \pm 6.43_b$	$92.58 \pm 0.38_c$
90	25	$1.27 \pm 0.15a$	6902.8_b	$3.77 \pm 0.30_a$	$400.30 \pm 1.21_{ab}$	$12.76 \pm 0.12_a$	$17.75 \pm 2.29_a$	$136.36 \pm 2.43_c$	$90.00 \pm 4.71_c$
90	40	$2.72 \pm 0.05_b$	7528.7_c	$23.7 \pm 0.80_b$	$354.45 \pm 1.62_a$	$24.70 \pm 0.53_d$	$64.56 \pm 0.34_c$	$118.18 \pm 6.43_b$	$88.69 \pm 4.21_{bc}$
90	55	$2.88 \pm 0.15_b$	7431.5_c	$23.5 \pm 1.32_b$	$1259.50 \pm 1.48_c$	$22.62 \pm 0.60_c$	$46.47 \pm 3.65_{bc}$	$127.27 \pm 1.44_b$	$85.71 \pm 6.43_b$
110	25	$1.41 \pm 0.13_a$	6417.9_a	$3.82 \pm 0.06_a$	$427.85 \pm 6.57_b$	$11.88 \pm 0.36_a$	$9.93 \pm 0.52_a$	$145.45 \pm 6.43_{cd}$	90.62 ± 4.41c
110	40	$3.08 \pm 0.02_{bc}$	7424.6_c	$24.2 \pm 0.32_b$	$368.65 \pm 1.63_a$	$22.78 \pm 0.69_c$	$84.85 \pm 3.77_d$	$95.45 \pm 6.43_a$	$90.45 \pm 0.64_c$
110	55	$3.13 \pm 0.06_{bc}$	7135.1_{bc}	$23.2 \pm 0.85_b$	$1368.30 \pm 1.98_c$	$15.14 \pm 0.04_{ab}$	$33.78 \pm 4.65_b$	$131.18 \pm 4.32_{bc}$	$51.66 \pm 2.35_a$

[a] DD: Degree of deamidation.
[b] DH: Degree of hydrolysis.
[c] S_0: surface hydrophobicity.
[d] EAI: emulsification index.
[e] ESI: Emulsification stability.The data with different letters in the same column are significantly different ($p < 0.05$).

2.3. Degree of hydrolysis (DH) and degree of deamidation (DD)

Degree of deamidation were determined according to our published method (Liao et al., 2011). Degree of hydrolysis was defined as the percentage of peptide bonds cleaved during the reaction, which was calculated from the ratio of free amino groups to the total number of peptide bonds in soluble factions during deamidation, according to the method described by Kong, Zhou, and Qian (2007). The determination of free amino groups in samples was carried out as follows: 0.25 mL of soluble fractions obtained from centrifugation was mixed with 2 mL of 0.2 M sodium phosphate buffer (pH 8.0) in the presence of 1% SDS and 2 mL of 0.1% trinitrobenzenesulfonic acid, followed by incubation in the dark for 60 min at 50 °C. The reaction was quenched by adding 4 mL of 0.1 M HCl and the absorbance was read at 340 nm. L-leucine solutions of 0.15–l.5 mM were used as standard. The total number of peptide bonds in suspensions was obtained by the hydrolysis of relevant soluble factions under vacuum in 6 mol/L HCl for 24 h at 110 °C in sealed tubes.

2.4. Zeta potential and dynamic light scattering (DLS)

Zeta potential and the mean hydrodynamic diameter of samples were determined according to the method described by Zhang et al. (2010). Zeta potential was measured by a laser doppler velocimetry and phase analysis light scattering (M3-PALS) technique using a Malvern Zetasizer Nano ZS (ZEN 3600) instrument (Malvern Instruments Ltd., Malvern, Worcestershire, UK). The mean hydrodynamic diameter of samples was measured by a dynamic light scattering technique using a Zetasizer Nano ZS (Malvern Instruments Ltd., Malvern, Worcestershire, UK) equipped with a 4 mW helium/neon laser at a wavelength output of 633 nm. The samples were diluted to about 2 mg/mL with 0.01 mol/L phosphate buffer (pH 5.03). One milliliter of each diluted sample was put in an electrophoresis cell (Model DTS 1060C, Malvern Instruments Ltd., Malvern, Worcestershire, UK). The temperature of the cell was maintained at ambient temperature. The data was the average values of three measurements performed with three individually prepared protein dispersions.

2.5. Surface hydrophobicity

Surface hydrophobicity was determined using l-anilino-8-naphthalene sulfonate (ANS^-) as a fluorescence probe with modifications described by Haskard and Li-Chan (1998). 4 mL of protein soluble fractions at successive concentration (0.005%, 0.01%, 0.02%, 0.05%, 0.1%) (w/v) were prepared in 10 mM phosphate buffer (pH 7.0). 20 μL of 8×10^{-1} M ANS^- stock solution was added into protein solutions. The mixtures were shaken in a vortex mixer for 5 s. Fluorescence intensity (FI) was measured at wavelengths of 390 nm (excitation) and 470 nm (emission) using a RF-5301 PC spectrofluorometer (Shimadzu Corp., Kyoto, Japan) at 26 ± 0.5 °C, with a constant excitation and emission slit of 5 nm. The FI for each sample with probe was then computed by subtracting the FI attributed to protein in buffer. The initial slope of the FI versus protein concentration was calculated by linear regression analysis and used as an index of surface hydrophobicity.

2.6. Evaluation of emulsification characteristics

Emulsification activity index (*EAI*) and emulsion stability index (*ESI*) of samples were determined by the turbidimetric technique of Agyare, Addo, and Xiong (2009) with some modifications. Corn oil (10 mL) and protein solution (4.0 g/L sample in 0.01 mol/L phosphate buffer, pH 4.4, 30 mL) were homogenized with an T25 Ultra Turrax-homogenizer (IKA Works Inc., Wilmington, NC) at a speed of 20, 000*g* for 1 min at 30 °C. 1 mL of the emulsion was diluted serially by 1/50–1/500, using 1.0 g/L sodium dodecyl sulphate (SDS) solution. Absorbance were recorded at 500 nm (A_{500}) using a Spectrumlab 22PC spectrophotometer (Shanghai Lengguang Technology Co. Ltd., Shanghai, PRC). *EAI* was calculated as below:

$$\zeta = \frac{2.303\ \mathrm{N}\ \mathrm{A}_{500}}{\mathrm{L}}; \quad EAI\ (\mathrm{m}^2/\mathrm{g}) = \frac{2\zeta 10^{-4}}{\mathrm{C}\phi}$$

where A_{500} is the absorbance at 500 nm; Φ is the volume fraction of dispersed phase; L is the light path in meters (1 cm); C is the concentration of protein before the emulsion is formed (g/mL); N is diluted folds; ζ is the evaluation of turbidity by emulsion solution of samples.

Emulsion stability index (*ESI*) was determined by placing aliquots of emulsion (10 mL) inside 10.0 mL cylinders immediately after preparation. At 0 and 30 min following emulsion preparation, 0.1 mL samples were pipetted and diluted 100 fold prior to turbidity measurements. *ESI* was calculated as follows:

$$ESI\ (\mathrm{min}) = \frac{\zeta_0 \Delta \mathrm{T}}{\Delta\zeta}$$

where Δζ is the change in turbidity after the time interval ΔT (30 min).

2.7. Evaluation of foaming property

Foaming property was determined by the method described by Popineau, Huchet, Larré, and Bérot (2002) with modifications. Protein solution (10.0 g/L sample in 0.01 mol/L phosphate buffer, pH 4.4) was homogenized with an T25 Ultra Turrax-homogenizer

(IKA Works Inc., Wilmington, NC) at a speed of 20, 000*g* for 1 min at 30 °C. Foaming capacity was calculated as the percentage increase in volume of protein dispersion upon mixing, whilst foaming stability was estimated as the percentage of foam volume remained after 30 min.

2.8. Size exclusion-high-performance liquid chromatography (SE-HPLC)

SE-HPLC was performed using a Biosep-*SEC*-S4000 size-exclusion analytical column (7.8 × 300 mm, Phenomenex Inc., Torrance, CA, US). All samples (1.0 mg/mL) were extracted with a 0.05 mol/L sodium phosphate buffer (pH 4.4) and loaded (10 μL) on the column. The elution solvent was (1:1, v/v) acetonitrile (ACN)/water containing 0.5 mL/L trifluoroacetic acid, with the flow rate of 0.8 mL/min at 25.0 °C according to the method described by Wang, Wei, Li, Bian, and Zhao (2009). The elution profiles were divided into two fractions using the lowest absorbance reading between the two peaks as the cut-off point. The peaks (MW > 90 kDa; retention time < 14.5 min) corresponded to the amount of polymeric fraction (glutenin). The second peaks (MW < 90 kDa; retention time > 14.5 min) could be assigned to the amount of gliadin fraction.

2.9. Sodium dodecyl sulfate-polyacrylamide gel electrophoresis (SDS-PAGE)

Freeze-dried modified samples were respectively dissolved in distilled water to 2 mg/mL. 20 μL of each sample was mixed with 10% (w/v) SDS and 1% (v/v) β-mercaptoethanol, then denatured in boiling water for 10 min, centrifuged at 10, 000*g* for 3 min. 10 μL of the denatured sample was loaded onto a homogeneous phastgel (DYCZ-24DN, Beijing liuyi instrument factory, PRC) and tested according to the method of Laemmli, Beguin, and Gujer-Kellenberger (1970) using 12% acrylamide separating gel and 5% acrylamide stacking gel. Samples were prepared in Tris-glycine buffer (pH 8.8), containing 1.5% SDS and the gel sheets were stained with Coomassie brilliant blue R-250 for 1 h at 30 °C.

2.10. Fourier transform infrared (FTIR) spectroscopy

FTIR spectra of samples were recorded according to the method reported by Liao et al. (2011) at 400–4000 cm^{-1} wavenumbers with resolution of 4 cm^{-1} using a Nicolet 8210E FTIR spectrometer (Nicolet, WI, USA) equipped with a deuterated triglycine sulphate detector. The spectrometer was continuously purged with dry air from a Balston dryer (Balston, MA). Sample powder (kept at an ambient temperature) measured was 1 mg sample per 200 mg of KBr. After homogenizing with an agate mortar and pestle, the powder was pressed into pellets (1–2 mm thick films) with a 15-ton hydraulic press. FTIR spectra were obtained in the range of wave number from 400 to 4000 cm^{-1} during 128 scans, with 2 cm^{-1} resolution (Paragon 1000, Perkin–Elmer, USA). The interpretation of the changes in the overlapping amide I band (1600–1700 cm^{-1}) components, was made possible by deconvolution using Peak-Fit v4.12 software (SPSS Inc.).

2.11. Intrinsic fluorescence spectroscopy

The tryptophan emission fluorescence spectra were recorded using an F-4600 fluorometer (Hitachico., Tokyo, Japan) by the method of Wong et al. (2012). Protein solutions (1 mg/mL) were prepared at pH 4.4 in final phosphate buffer (0.01 mol/L). The fluorescence spectra of the samples were all recorded using an excitation wavelength of 295 nm, recorded from 300 to 400 nm at a constant slit of 5 nm and a scanning speed of 1200 nm/min.

2.12. Statistical analysis

All tests were performed in triplicate. Analysis of variance and significant difference tests were conducted to identify differences among means using the LSD multiple-range test with SPSS software (version 13.0 for Windows, SPSS Inc., Chicago, IL). The significance level (p) was set at 0.05. Agglomerative hierarchical clustering (AHC) analysis and principal component analysis (PCA) were performed for data classification and dimensionality reduction by using the statistical software XL-Stat 2015 (Addinsoft, Barcelona, Spain). AHC was performed on functional, structural and physicochemical profiles to both group the most similar samples by using Pearson's correlation coefficient and agglomeration via an unweighted pair-group average and to distinguish dissimilarity using the Euclidean distance dissimilarity matrix and agglomeration method of Ward. PCA and Pearson's linear correlation ($p < 0.05$) were used to test the relationship between the results obtained in the functional, structural, physicochemical and deamidation tests.

3. Results and discussion

3.1. Physicochemical analysis

Fig. 1 summarizes the physicochemical characteristics of the deamidated wheat gluten at three degrees of deamidation (~25%, ~40% and ~55%) produced by three concentrations of citric acid (3.93×10^{-5}, 3.14×10^{-3} and 2.36×10^{-2} mol/L) (CDWGs), which were subjected to different hydrothermal treatments (70 °C for 2 h (**I**), 90 °C for 1 h (II) and 110 °C for 40 min (III)) (see Table 1 in the supplementary material). The degree of hydrolysis (DH), zeta potential and particle hydrodynamic diameter are shown in Table 1 for the nine samples. At the same hydrothermal temperature, the zeta potential depended on the degree of deamidation (DD), but conversely, the zeta potential slightly decreased when DD was higher than 40%. At the same degree of deamidation (DD) produced by different temperatures but the same acid concentration, the value of the zeta potential non-significantly ($p < 0.05$) increased with an increase in temperature. For example, for 40% DD, the zeta potential was 22.2 mv for the sample treated at 70 °C for 2 h (CDWGI-40), 23.7 mv at 90 °C for 1 h (CDWG II-40) and 24.2 mv at 110 °C for 40 min (CDWGIII-40). Actually, the acid concentration was increased with temperature, so the zeta potential value should increase with the acid concentration in the system because deamidated carboxyl groups were protonated and the cationic amino groups should occupy the surface in an acid solution. However, the actual trend of the zeta potential was not as we predicted. This may imply that other mechanisms in addition to deamidation occurred, such as molecule and conformational changes. Accordingly, it could be speculated that the availability of H^+ to react with wheat gluten amide groups was not governed by the acid concentration used, but probably depended on the actual conformation and the acting temperature. The zeta potential is commonly used to indicate the stability of a protein suspension with respect to the charge density and electrostatic repulsion of the protein (Jachimska, Wasilewska, & Adamczyk, 2008). Wheat gluten contains a large percentage (approximately 50%) of uncharged amino acid residues (Gln and Asn residues) in gliadins and glutenins (Wagner et al., 2011). As previously mentioned, deamidation would have a pronounced effect on the charge density and the resultant electrostatic repulsion of the protein (Zhao et al., 2011). We therefore chose the zeta potential as the first factor to evaluate the differences in the modified wheat gluten proteins that had a similar degree of deamidation (DD) produced by different deamidation processing conditions.

The DH of CDWGs behaved somewhat similarly to the zeta potential, but showed a tendency to hydrolyse peptide bonds when the DD was higher than 40%. At the same temperature, the DH was increased with an increase in the degree of deamidation. At the same degree of deamidation, as the temperature increased, the DH decreased. Matsudomi, Kato, and Kobayashi (1982) reported that acid-modified gluten at >40% deamidation might exhibit a conformational change due to the cleavage of peptide linkages in the gluten molecule and conformational changes due to S-S disruption from the acid hydrolysis of gluten. For mild acid-treated soybeans, they reported the hydrolysis of peptide bonds became important at a deamidation level >10%, (Matsudomi et al., 1985). These explanations led us to speculate that a stronger hydrothermal treatment exposed more amide groups because of the rupturing of the conformation by parts of H^+ via the acid hydrolysis of the peptide bonds in the protein. It was also apparent that all of the aggregates in the CDWGs (Table 1) shifted considerably towards a higher hydrodynamic diameter at the highest acid concentration in the three different temperature treatments. Specifically, the samples that had a DD >40% had a particle size that was the minimum, but the hydrodynamic diameter of the 55% samples was 3-fold higher than that of the 40% samples (from ~400 nm at 40% DD up to ~1300 nm at 55% DD). This observation indicated that the wheat gluten was largely dissociated and its conformation was thoroughly unfolded and fully branched when prepared with a severe hydrothermal treatment. It is noteworthy that the hydrodynamic diameter of the aggregates in the CDWGs prepared at the same acid concentration increased with an increase in the temperature at which they were prepared. The higher energy of the H^+ that split the protein backbone chains at a higher temperature and the more open structure produced by the greater electrostatic repulsion due to deamidation might be the main reasons that the aggregates significantly ($p < 0.05$) expanded in wheat gluten, as indicated by the striking increase in the hydrodynamic diameter.

3.2. Comparison of functional properties

Protein functionality is derived from the physicochemical characteristics, such as the molecular size, amino acid composition and sequence, conformation, net charge, and surface hydrophobicity. Any modification that alters one or more of these characteristics can also change the functional properties (Wagner & Gueguen, 1999). The emulsification and foaming characteristics of CDWGs were studied (Table 1) to further elucidate the differences in samples that had a similar DD but were prepared at different temperatures and pH values (acid concentrations). Surface hydrophobicity (S_0) was also determined and is shown in Table 1. The emulsification characteristics (EAI and ESI) and foaming capability were observed to exhibit a somewhat similar behaviour as the zeta potential increased. When DD was increased to 40%, the emulsification ability and emulsion stability were optimal and the foaming capability was the lowest. This result agreed with the results of Wu and Yang (1976) and Liao et al., (2010a) which showed that samples had a higher foaming capacity at a lower degree of deamidation, suggesting that an excessive increase in the degree of deamidation did not increase the foaming capacity, probably because a large amount of carboxyl was produced that enhanced the electrostatic interactions and produced bulk molecules with a large hydrodynamic diameter (see Section 3.1). The latter affected the balance of the hydrophobic and hydrophilic groups as a consequence of the loss of the adsorption and anchorage of proteins at the air-water interface (Wagner & Guéguen, 1999).

Surface hydrophobicity is the protein characteristic that is most likely to define its surface behaviour and consequently its emulsifying properties. A positive correlation between surface hydrophobicity, surface tension, and the emulsifying activity index has been reported (Wagner & Guéguen, 1999), which occurs because the exposed hydrophobic patch on the protein surface facilitates protein binding on the hydrophobic oil droplet surface, and then, the proteins could aggregate via the surface hydrophobic patches to form films around the oil droplet surfaces (Lam & Nickerson, 2015; Takeda, Matsumura, & Shimizu, 2001). In this study, the surface hydrophobicity and EAI value of all samples showed a positive linear correlation, as predicted (the linear fit was given by $y = 0.0083x + 40.992$, $R^2 = 0.7478$, where x is the surface hydrophobicity and y is the EAI value – data not shown). As shown in Table 1, the surface hydrophobicity of deamidated wheat gluten decreased as the acid concentration and strength of the hydrothermal treatment increased. At the same temperature, when the degree of deamidation was increased from 25% to 40%, the surface hydrophobicity increased significantly ($p < 0.05$), indicating that the increase in the DD exposed the protein hydrophobic regions. However, at the same degree of deamidation, the surface hydrophobicity decreased with an increase in temperature, probably because thermal denaturation induced the exposure of thiol groups, which caused the deamidated wheat gluten to aggregate (Lam & Nickerson, 2015). Furthermore, when the deamidation degree was increased from 40% to 55%, the EAI and ESI of the deamidated wheat gluten also decreased, which demonstrated that extensive protein hydrolysis during chemical deamidation reactions prevented the formation of a continuous protein and stable film at the oil/water interface because of the loss of the globular structure and the optimum size of the peptides (Chan & Ma, 1999).

3.3. Comparison of conformation changes and molecular weight distribution

3.3.1. Molecular weight distribution

The appropriate degree of dissociation of the protein structure and the simultaneous unfolding of the polypeptide chains of its subunits markedly improved its solubility and surface active properties. This structural modification could be induced by various environmental factors, such as the ionic strength, pH, or temperature, or by chemical treatment (Wagner & Guéguen, 1999). We have observed that functional properties of deamidated wheat gluten when prepared with similar controlled DD but prepared at different temperature and pH (acid concentration) exhibited significantly ($p < 0.05$), as well as the incomplete availability of H^+ to catalyse amide groups of wheat gluten due to the increasing participation of H^+ to split protein peptide bonds activated by higher temperatures (see Section 3.2). Thus, we expected to find secondary and tertiary conformation changes together with an altered molecular weight distribution, which would further confirm the assumption that the availability of H^+ to catalyse amide groups of wheat gluten was dependent on the conformation and acting temperature. SDS-PAGE (Fig. 2) and SE-HPLC (Fig. 3A, B & C) on the CDWGs to were used to determine changes in the molecular weight distribution of deamidated wheat gluten. FTIR analysis (Table 2) and endogenous fluorescence spectroscopy (Fig. 3D, E & F) were conducted to further investigate the differences in the secondary and tertiary conformation of the CDWGs after processing.

Fig. 2 indicates a clear difference in the nature of the subunit bands as well as their intensity among the CDWGs that had the same DD but were prepared at different temperatures. For CDWGs with a DD of 25% (lane 1, 4 and 7) compared to CDWGs prepared at 70 °C for 2 h (**I**) (lane 1), the intensity of one peptide band of ω-gliadins and four peptide bands of LMW-GS (Groups B&C) (with molecular weights of 29.0 kDa to 66.4 kDa) were observed to generally decrease as the temperature increased (see the three arrows beside lane 1 in Fig. 2). Spontaneously and interestingly, the intensity of several bands below LWM-GS (less than

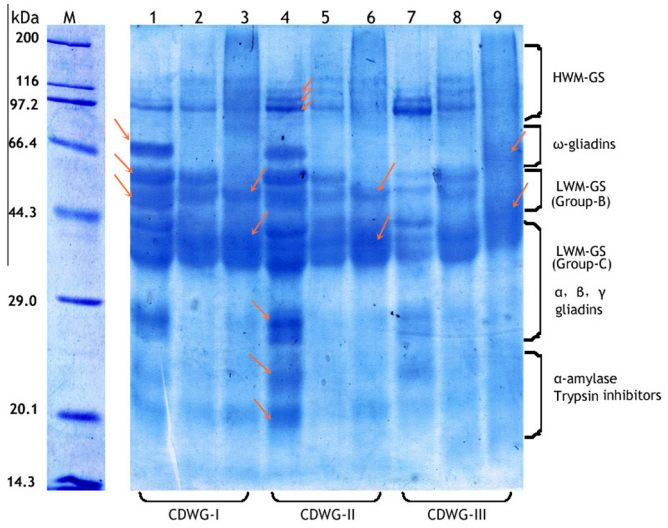

Fig. 2. SDS-PAGE analysis of CDWGs at three levels of degree of deamidation obtained by different deamidation processing conditions (70 °C (CDWG-I), 90 °C (CDWG-II) and 110 °C (CDWG-III)). Lane 1–3 were CDWGI-25, CDWGI-40 and CDWGI-55 respectively; Lane 4–6 were CDWGII-25, CDWGII-40 and CDWGII-55 respectively; Lane 7–9 were CDWGIII-25, CDWGIII-40 and CDWGIII-55 respectively.

29.0 kDa, see the three arrows beside lane 4 in Fig. 2) and three bands above ω-gliadins were apparently increased, but the former largely disappeared when temperature was increased to 110 °C (see the six arrows beside lane 4 in Fig. 2). In agreement with Matsudomi et al. (1982) that a DD of 40% was a critical point at which conformational changes were induced, two observations are evident for CDWGs at 40% DD. (1) Compared to the subunit bands of CDWG at 25% DD, the intensity of the higher molecular weight bonds (>29.0 kDa) apparently weakened when the temperature was changed from 70 °C for 2 h (**I**) (lane 2) to 90 °C for 1 h (II) (lane 5). This observation agreed with the trend in the HD (Table 1), further suggesting that breakage of the peptide bonds did not only occur in HWM-GS but also in gliadins and LMW-GS at higher temperatures (Lan Liao, Wang, & Zhao, 2013). (2) However, this band pattern was not maintained when the DD was higher than 40% (lane 3, 6 & 9) or the temperature was increased to 110 °C for 40 min (III)) (lane 8). Compared to the CDWG at 40% DD, an apparent increase in the aggregation state was observed when CDWGs at 55% DD were prepared at higher temperatures (lane 3, 6 & 9). Two newly formed bands (see the arrows beside lane 9 in Fig. 2), which did not appear in CDWGs prepared at 70 °C and 90 °C (lane 3 and 6), were evident. These might be new aggregates produced by crosslinking the two bands near 44.3 kDa (see the two arrows beside lane 3 & 6 in Fig. 2); however, this hypothesis certainly needs to be further investigated. As previously mentioned, wheat gluten is a mixture of glutenins (network polypeptides) and gliadins (monomers) that associate via non-covalent interactions. Schofield, Bottomley, Timms, and Booth (1983) indicated that at 100 °C, the glutenins and gliadins appeared to crosslink with each other or with themselves. Thus, these results indicated that the heat treatment caused polymerization of the protein accompanied by the unfolding of the wheat gluten due to acid hydrolysis of the peptide backbone and negative electrostatic repulsion due to deamidation.

SDS-PAGE was performed under reducing conditions and yielded information about the distribution of the gluten in gliadin subunits after heating-acid treatments. SE-HPLC was performed under neutral unreduced conditions, to provide more information about the changes in the molecular weight distribution of the glutenins and gliadins after treatment. Fig. 3 shows the SE-HPLC

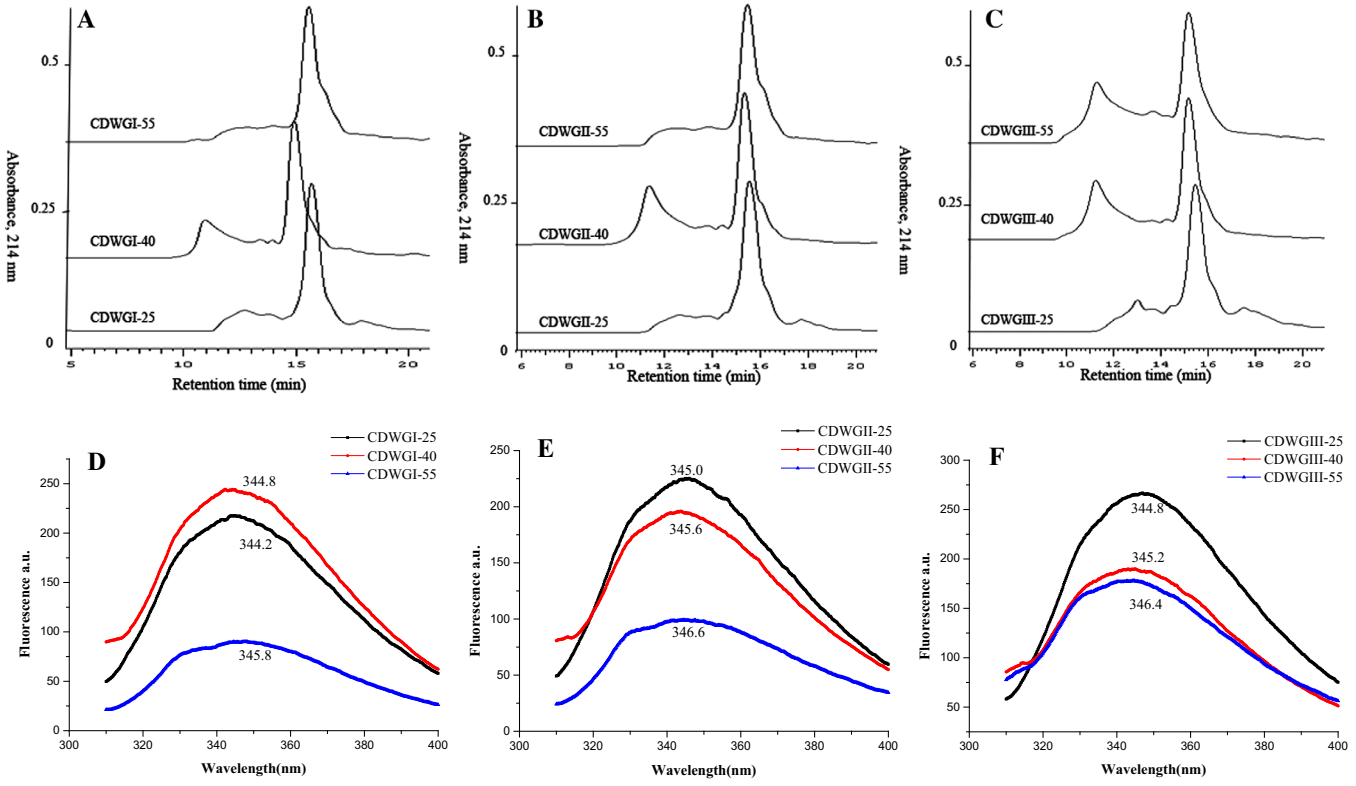

Fig. 3. SEC-HPLC profiles (A, B and C) and endogenous fluorescence scanning (D, E and F) of CDWGs at three levels of degree of deamidation obtained by different deamidation processing conditions (70 °C (CDWG-I), 90 °C (CDWG-II) and 110 °C (CDWG-III)), respectively.

Table 2
Secondary structure of CDWGs at three levels of degree of deamidation obtained by different deamidation processing conditions (70 °C (CDWG-I), 90 °C (CDWG-II) and 110 °C (CDWG-III)).

Temperature (°C)	DD[b] (%)	Intermolecular β-sheet aggregation extended		Intramolecular aggregation extended β-sheet (hydrated)		α-Helix		β-Turn		Extended β-sheet		α-Helix/β-sheet
		Frequency (cm^{-1})	Content [a] (%)	Frequency (cm^{-1})	Content [a] (%)	Frequency (cm^{-1})	Content [a] (%)	Frequency (cm^{-1})	Content [a] (%)	Frequency (cm^{-1})	Content [a] (%)	
70	25	1604.5	11.09	1635.4	32.61	1652.7	35.31	1679.7	19.42	1693.2	1.57	0.78
70	40	1604.4	13.45	1633.5	31.47	1652.7	34.91	1679.7	18.74	1693.3	1.43	0.75
70	55	1604.5	11.61	1629.6	28.43	1654.7	36.07	1679.7	22.10	1693.2	1.79	0.86
90	25	1604.5	10.81	1629.6	29.14	1650.8	36.77	1679.7	21.50	1695.2	1.78	0.88
90	40	1604.5	10.19	1635.4	32.41	1652.7	35.63	1679.7	20.19	1693.2	1.58	0.81
90	55	1604.5	11.00	1629.6	29.29	1654.7	35.41	1679.7	22.52	1693.2	1.78	0.84
110	25	1604.5	10.99	1629.6	28.15	1654.7	36.53	1679.7	22.51	1693.2	1.82	0.89
110	40	1604.5	12.89	1633.5	31.69	1652.7	34.84	1679.7	19.00	1693.2	1.58	0.75
110	55	1604.5	13.46	1633.5	28.43	1650.8	35.79	1672.1	20.76	1693.2	1.56	0.82

[a] The percentage of secondary structure content is estimated as the corresponding area as a percentage of the total amide I band area.
[b] DD: Degree of deamidation.

chromatogram profiles, and Fig. 1 in the supplementary material illustrates the area percentages of the peaks of two fractions (glutenins and gliadins) to the peaks of wheat gluten as a function of the hydrothermal temperature and degree of deamidation (see Fig. 1 in the supplementary material).

The following observations can be made from Fig. 3(A, B & C) and Fig. 1 in the supplementary material. (1) At 70 °C and 90 °C, compared with the chromatographic profile of CDWG-25, the elution time of the gluten in peak was generally shorter and the glutenins peak areas of CDWG-40 significantly increased and then had an decreasing trend when the DD was increased to 55%. (2) The area percentages for the gliadin peaks at the 70 °C and 90 °C increased, following a significant reduction when the DD was increased 55%. (3) When heated to 110 °C, the peaks of the polymeric proteins showed a progressively longer retention time (from 15.15 min for 25% DD to 15.62 min for 55% DD) and a lower area percentage (from 82.08% for 25% DD to 48.39% for 55% DD). (4) A significant ($p < 0.05$) increase of the area percentage of the gliadin peaks was observed as the DD increased from 25% to 55% (from 17.62% for 25% DD to 51.56% for 55% DD).

These molecular properties of the wheat gluten components (gliadins and glutenins), as well as the results from SDS-PAGE, DLS and degree of hydrolysis, led to the hypothesis that for carboxylic acid deamidation, a limited amount of H^+ at a higher temperature (~90 °C) could catalyse the deamidation of amide groups without providing excess H^+ to hydrolyse peptide bonds.

3.3.2. Conformational changes

To gain a deeper understanding of CDWGs prepared at the same DD but at different pH and temperatures, FTIR was used to investigate differences in the secondary structures of CDWG-I (25, 40, 55), CDWG-II (25, 40, 55) and CDWG-III (25, 40, 55) by analysing the amide I (1600–1700 cm^{-1}) that indicated the secondary structure in the sample spectra. The contents of the secondary structure components were calculated (Table 2). Deconstruction of the amide I region of the samples indicated five components located at 1604, ~1635, ~1652, 1679 and 1693 cm^{-1}, representing intermolecular β-sheets of protein aggregation, intramolecular extended β-sheets (hydrated), an α-helix, a β-turn and an extended β-sheet, respectively.

Table 2 shows that an increase in the DD of the CDWGs was generally associated with a reduced α-helix content, while the β-sheet content was increased at the same temperature. When temperature was increased from 70 °C to 110 °C, the β-turn content in deamidated wheat gluten was higher at the same DD, which was in line with the trends in the zeta potential and HD (Table 1), further verifying that a higher temperature caused greater exposure of the buried residues and greater electrostatic repulsion and hydrogen bondings. The ratio of α-helices to β-sheets represented the molecular flexibility of a protein. With an increase in temperature from 90 °C to 110 °C, the α-helix to β-sheet ratio of CDWGs at the same DD decreased, which demonstrated that a higher temperature produced a more flexible structure in modified wheat gluten.

Fig. 3D, E & F shows the endogenous fluorescence emission spectra of CDWGs prepared under different processing conditions. When DD was increased from 25% to 55% at processing temperatures of 70 °C, 90 °C and 110 °C, the observed red-shift in λ_{max} indicated a significant change in the tertiary structure due to an expansion of the wheat gluten structure and the exposure of hydrophobic groups with an increase in the degree of deamidation (Liao et al., 2013). At temperatures of 90 °C and 110 °C, the endogenous fluorescence emission spectra of protein generally indicated a red-shift with increasing temperature at the same DD, demonstrating that heating caused a slight unfolding of the protein molecular structure. Moreover, at the same DD, the λ_{max} at 90 °C was greater than at 70 °C or 110 °C. This protein behaviour was in line with its surface hydrophobicity and emulsion properties, as well as the SDS-PAGE results, suggesting that the structural rearrangements of protein at 90 °C evidenced the largest unfolding of the structure.

3.4. Agglomerative hierarchical clustering (AHC) and principal component analysis (PCA)

The above results qualitatively indicated a relationship between the degree of aggregation and functional and structural properties due to an alteration in the degree of deamidation by controlling the pH and temperature. Agglomerative hierarchical clustering (AHC) analysis and principal component analysis (PCA) were used to establish sample groupings and quantitatively determine specific relationships based on the chemometrics of pre-determined parameters regarding the functional, structural and physicochemical properties listed in Tables 1 and 2 (altogether 19 variables and 9 samples). Cluster analysis (CA) separates data into mutually exclusive cohorts by minimizing within-group dissimilarity, while simultaneously maximizing the between-group dissimilarity. Dendrogram linkages effectively depict the agglomeration sequence and the degree of similarity between clusters containing similar samples. In this study, we used two agglomerative hierarchical clustering (AHC) methods, one based on the proximity dissimilarity of the Euclidean distance using Ward's agglomeration method (Fig. 4A) and the other on the proximity similarity of the Pearson

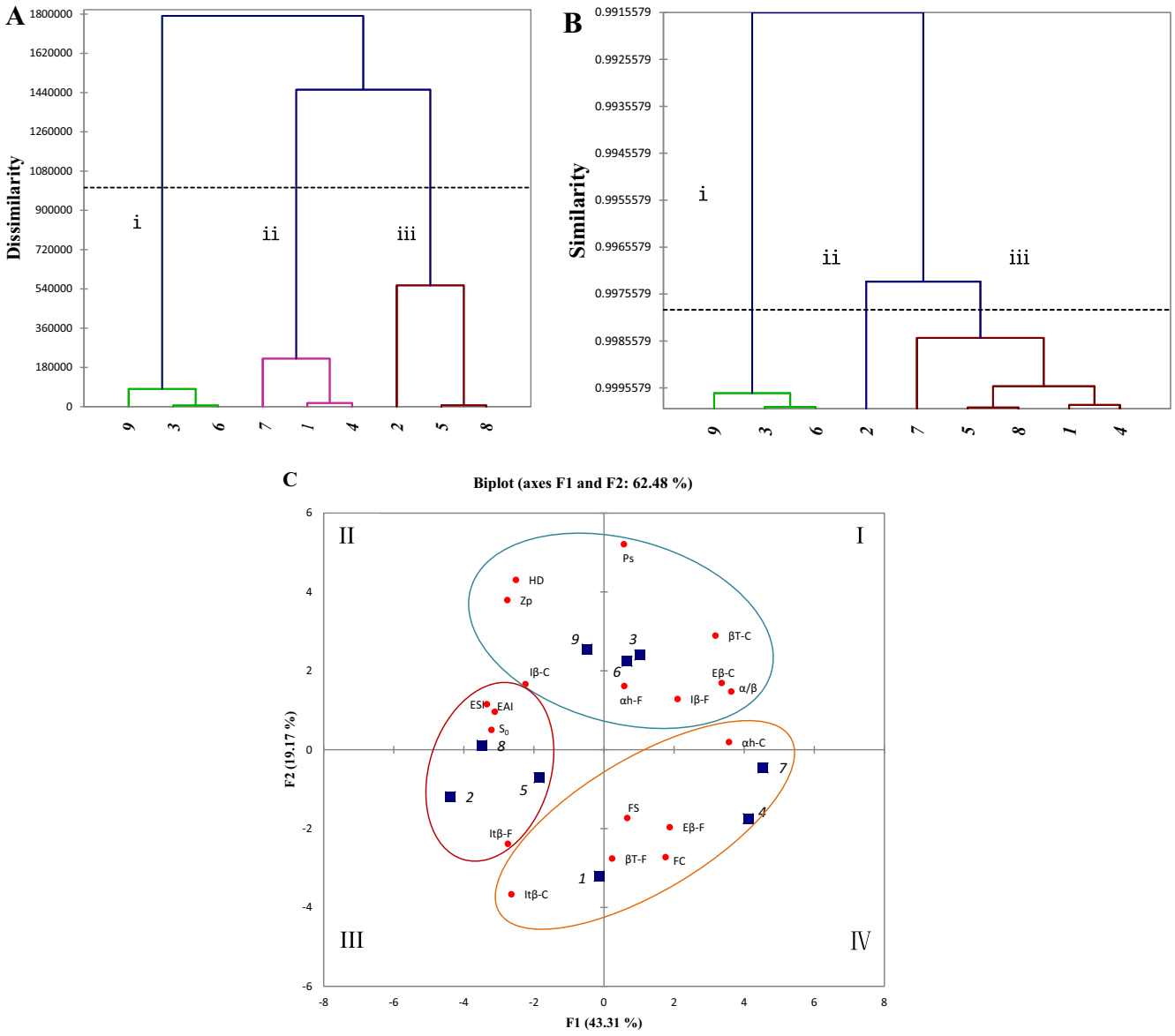

Fig. 4. Dendrograms from AHC of 9 samples (A & B) and plots of the PCA coefficients for samples and loading 19 variables (C). A, dissimilarity relationships between 9 samples are shown, as estimated by clustering analysis of functional, structural and physicochemical profiles of 9 samples. The Euclidean distance dissimilarity method and the agglomeration method of Ward were employed. B, similarity relationships between 9 samples are shown, as estimated by clustering analysis of functional, structural and physicochemical profiles. The Pearson correlation coefficient method and the agglomeration method of Unweighted pair-group average were employed. C, the Pearson' linear correlation ($p < 0.05$) was used. Sample names were indicated as follow: *1*, CDWGI-25; *2*, CDWGI-40; *3*, CDWGI-55;*4*, CDWGII-25; *5*, CDWGII-45; *6*, CDWGII-55; *7*, CDWGIII-25; *8*, CDWGIII-40; *9*, CDWGIII-55. Parts of variable names were abbreviated as follow: Zp, Zeta potential; Ps, Particle size; FC, Foaming capacity; FS, Foaming stability; Iβ-F, Intermolecular β-sheet aggregation extended (Frequency); Iβ-C, Intermolecular β-sheet aggregation extended (content); Itβ-F, Intramolecular aggregation extended β-sheet (hydrated) (Frequency); Itβ-C, Intramolecular aggregation extended β-sheet (hydrated) (content); αh-F, α-helix (Frequency); αh-C, α-helix(content); βT-F, β-turn (Frequency); βT-C, β-turn (content); Eβ-F, Extended β-sheet (Frequency); Eβ-F, Extended β-sheet (content); α/β, α-helix/β-sheet.

correlation coefficient using the Unweighted pair-group average agglomeration method (Fig. 4B). The dendrograms generated by both AHCs identified three sample cohorts with similar characteristics, but were visibly distinct. As shown in Fig. 4A, Group i predominantly included samples 3, 6 and 9, which had a 55% DD obtained at 2.36×10^{-2} mol/L. Group ii included samples 1, 4 and 7, which had 25% DD and showed a slight linkage to group iii, which included samples 2, 5 and 8, which had 40% DD prepared at 3.14×10^{-3} mol/L. A unique pattern of group linkages dependent on the other properties of samples was evident. These surprising observations indicted that the pH had a decisive influence on the deamidation of wheat gluten. The average distance to the centroid for Group iii (406.08) was almost double that of Group i (256.09) and Group ii (160.00) and was analogous with the designation of a critical DD of 40% by Matsudomi et al. (1982) and the SDS-PAGE results (Fig. 2). Unweighted pair-group algorithm using Pearson's correlation coefficient was used to construct a dendrogram that indicated the structure in a pairwise similarity matrix. Further intriguing information based this algorithm is evident in Fig. 4B, which shows that Group i (samples 3, 6 and 9) was predominantly distinct from samples 2, 7, 5, 8, 1 and 7, which were much more similar to each other. A possible explanation might be that samples 3, 6 and 9 were intrinsically differentiate from samples of 2, 7, 5, 8, 1 and 7 in conformation and molecular weight distribution.

The relationship between the samples and the variables unique to each other can be further judged by PCA. The PCA graph of the physicochemical and functional and secondary structural

properties are shown in Fig. 4C. The first principal component (CP1) accounted for 43.31% of the total range, while the second principal component (CP2) accounted for 19.17%. Therefore, CP1 and CP2 together accounted for 62.48% of the total range. Fig. 4C shows that the degree of hydrolysis (HD), zeta potential (Zp), EAI, ESI, S_0 and intermolecular β-sheet aggregation extended (content) (Iβ-C) were located in quadrant II. The other parameters, including the secondary structural factors, particle size (Ps) and foaming ability (FS & FC), were located in quadrants I and IV. The second component (CP2) indicated that the parameters HD and Ps were highly significant. The most important parameters on axis CP1were the α-helix content (αh-C), S_0 and ESI. This figure indicates that the EAI, ESI and S_0 vectors are located together and similarly affect the emulsification behaviour of samples 2, 5, 8. Similar effects of HD and Zp on the deamidation of sample 9 and of the α-helix frequency (αh-F) on samples 3 and 6 are evident. Surprisingly, the parameter β-turn frequency (βT-F) showed the best relationship (0.949, see Table 2 in the supporting information) with the foaming stability (Fs), influencing the deamidation of sample 1.

The PCA results were in accord with the AHC groupings. Based on the distribution of the samples in the loading plot, the dissimilarity group information from AHC indicated that samples 3, 6 and 9 were close to each other; samples 2, 5 and 8 were adjacent; and samples 1, 4 and 7 were related to each other by the variables FS, FC, βT-F and the extended β-sheet frequency (Eβ-F). Samples 3, 6 and 9 were affected mainly by the HD, Zp, Ps, α-helix/β-sheet (α/β) and β-sheet contents, illustrating that samples 3, 6 and 9 had a well extended and branched conformation. Samples 2, 5 and 8 showed that the emulsification ability and S_0 affected the responses because they had the highest values for each hydrothermal treatment.

4. Conclusion

This comparison provide qualitative and quantitative evidence that the carboxylic acid deamidation processing conditions, including the pH and temperature, have a significant effect on the physicochemical and functional properties, as well as the structural properties, of wheat gluten. AHC and PCA qualitatively demonstrated that pH had the greatest influence on the deamidation of wheat gluten. At a moderate citric acid concentration, CDWG of 40% DD (CDWG-40) showed better emulsifying and foaming properties for all temperatures and no significant changes in the protein structure. Furthermore, conformational changes at temperatures higher than 90 °C and higher acid concentrations were observed along with significant protein aggregation, even though they were accompanied by the unfolding of the wheat gluten due to acid hydrolysis of the peptide backbone. We therefore proposed that the moderate deamidation conditions at temperatures not exceeding of 100 °C and an appropriate acid concentration were sufficient to unfold the protein structure and enhance electrostatic repulsion by promoting the flexibility of wheat gluten, eliminating excessive peptide bond breakage by excess H^+, which was activated at higher temperatures. These findings allow a better understanding of the deamidation of wheat gluten by carboxylic acid deamidation at different pHs and temperatures to produce different degrees of deamidation.

Acknowledgments

The authors would like to express their sincere gratitude to National Natural Science Foundation of China (No. 31201287) and Natural Science Foundation of Fujian Province of China (No. 2015J05067) for the financial support of this research.

Appendix A. Supplementary data

Supplementary data associated with this article can be found, in the online version, at http://dx.doi.org/10.1016/j.foodchem.2016.04.113.

References

Agyare, K. K., Addo, K., & Xiong, Y. L. (2009). Emulsifying and foaming properties of transglutaminase-treated wheat gluten hydrolysate as influenced by pH, temperature and salt. *Food Hydrocolloids, 23*(1), 72–81.

Berti, C., Roncoroni, L., Falini, M. L., Caramanico, R., Dolfini, E., Bardella, M. T., Elli, L., et al. (2007). Celiac-related properties of chemically and enzymatically modified gluten proteins. *Journal of Agricultural and Food Chemistry, 55*(6), 2482–2488.

Chan, W. M., & Ma, C. Y. (1999). Modification of proteins from soymilk residue (okara) by trypsin. *Journal of Food Science, 64*(5), 781–786.

Du, C. Y., Lin, S. K. C., Koutinas, A., Wang, R. H., Dorado, M. P., & Webb, C. (2009). A wheat biorefining strategy based on solid-state fermentation for fermentative production of succinic acid (vol 17, pg 8310, 2008). *Bioresource Technology, 100*(21). 5370-5370.

Haskard, C. A., & Li-Chan, E. C. (1998). Hydrophobicity of bovine serum albumin and ovalbumin determined using uncharged (PRODAN) and anionic (ANS-) fluorescent probes. *Journal of Agricultural and Food Chemistry, 46*(7), 2671–2677.

Jachimska, B., Wasilewska, M., & Adamczyk, Z. (2008). Characterization of globular protein solutions by dynamic light scattering, electrophoretic mobility, and viscosity measurements. *Langmuir, 24*(13), 6866–6872.

Kong, X., Zhou, H., & Qian, H. (2007). Enzymatic hydrolysis of wheat gluten by proteases and properties of the resulting hydrolysates. *Food Chemistry, 102*(3), 759–763.

Laemmli, U. K., Beguin, F., & Gujer-Kellenberger, G. (1970). A factor preventing the major head protein of bacteriophage T4 from random aggregation. *Journal of Molecular Biology, 47*(1), 69–85.

Lam, R. S., & Nickerson, M. T. (2015). The effect of pH and temperature pretreatments on the structure, surface characteristics and emulsifying properties of alpha-lactalbumin. *Food Chemistry, 173*, 163–170.

Lei, L., Zhao, Q., Selomulya, C., & Xiong, H. (2015). The effect of deamidation on the structural, functional, and rheological properties of glutelin prepared from *Akebia trifoliata* var. australis seed. *Food Chemistry, 178*, 96–105.

Liao, L., Liu, T. X., Zhao, M. M., Cui, C., Yuan, B. E., Tang, S., & Yang, F. (2010a). Functional, nutritional and conformational changes from deamidation of wheat gluten with succinic acid and citric acid. *Food Chemistry, 123*(1), 123–130.

Liao, L., Liu, T. M., Zhao, M. M., Zhao, H. F., & Cui, C. (2011). Aggregation behavior of wheat gluten during carboxylic acid deamidation upon hydrothermal treatment. *Journal of Cereal Science, 54*(1), 129–136.

Liao, L., Qiu, C. Y., Liu, T. X., Zhao, M. M., Ren, J. Y., & Zhao, H. F. (2010b). Susceptibility of wheat gluten to enzymatic hydrolysis following deamidation with acetic acid and sensory characteristics of the resultant hydrolysates. *Journal of Cereal Science, 52*(3), 395–403.

Liao, L., Wang, Q., & Zhao, M.-M. (2013). Functional, conformational and topographical changes of succinic acid deamidated wheat gluten upon freeze- and spray-drying: A comparative study. *LWT – Food Science and Technology, 50*(1), 177–184.

Liao, L., Zhao, M., Ren, J., Zhao, H., Cui, C., & Hu, X. (2010c). Effect of acetic acid deamidation-induced modification on functional and nutritional properties and conformation of wheat gluten. *Journal of the Science of Food and Agriculture, 90*(3), 409–417.

Matsudomi, N., Kato, A., & Kobayashi, K. (1982). Conformation and surface properties of deamidated gluten. *Agricultural and Biological Chemistry, 46*(6), 1583–1586.

Matsudomi, N., Sasaki, T., Tanaka, A., Kobayashi, K., & Kato, A. (1985). Polymerization of deamidated peptide fragments obtained with the mild acid hydrolysis of ovalbumin. *Journal of Agricultural and Food Chemistry, 33*(4), 738–742.

Morel, M. H., Redl, A., & Guilbert, S. (2002). Mechanism of heat and shear mediated aggregation of wheat gluten protein upon mixing. *Biomacromolecules, 3*(3), 488–497.

Popineau, Y., Huchet, B., Larré, C., & Bérot, S. (2002). Foaming and emulsifying properties of fractions of gluten peptides obtained by limited enzymatic hydrolysis and ultrafiltration. *Journal of Cereal Science, 35*(3), 327–335.

Qiu, C., Sun, W., Zhao, Q., Cui, C., & Zhao, M. (2013). Emulsifying and surface properties of citric acid deamidated wheat gliadin. *Journal of Cereal Science, 58*(1), 68–75.

Redondo-Cuenca, A., Villanueva-Suarez, M. J., & Mateos-Aparicio, I. (2008). Soybean seeds and its by-product okara as sources of dietary fibre. Measurement by AOAC and Englyst methods. *Food Chemistry, 108*(3), 1099–1105.

Schofield, J., Bottomley, R., Timms, M., & Booth, M. (1983). The effect of heat on wheat gluten and the involvement of sulphydryl-disulphide interchange reactions. *Journal of Cereal Science, 1*(4), 241–253.

Takeda, K., Matsumura, Y., & Shimizu, M. (2001). Emulsifying and surface properties of wheat gluten under acidic conditions. *Journal of Food Science, 66*(3), 393–399.

Wagner, J. R., & Guéguen, J. (1999). Surface functional properties of native, acid-treated, and reduced soy glycinin. 1. Foaming properties. *Journal of Agricultural and Food Chemistry, 47*(6), 2173–2180.

Wagner, J. R., & Gueguen, J. (1999). Surface functional properties of native, acid-treated, and reduced soy glycinin. 2. Emulsifying properties. *Journal of Agricultural and Food Chemistry, 47*(6), 2181–2187.

Wagner, M., Morel, M. H., Bonicel, J., & Cuq, B. (2011). Mechanisms of heat-mediated aggregation of wheat gluten protein upon pasta processing. *Journal of Agricultural and Food Chemisty, 59*(7), 3146–3154.

Wang, J. S., Wei, Z. Y., Li, L., Bian, K., & Zhao, M. M. (2009). Characteristics of enzymatic hydrolysis of thermal-treated wheat gluten. *Journal of Cereal Science, 50*(2), 205–209.

Webb, M. R., Naeem, H. A., & Schmidt, K. A. (2002). Food protein functionality in a liquid system: A comparison of deamidated wheat protein with dairy and soy proteins. *Journal of Food Science, 67*(8), 2896–2902.

Wong, H. W., Choi, S. M., Phillips, D. L., & Ma, C. Y. (2009). Raman spectroscopic study of deamidated food proteins. *Food Chemistry, 113*(2), 363–370.

Wong, B. T., Zhai, J., Hoffmann, S. V., Aguilar, M. I., Augustin, M., Wooster, T. J., & Day, L. (2012). Conformational changes to deamidated wheat gliadins and β-casein upon adsorption to oil–water emulsion interfaces. *Food Hydrocolloids, 27*(1), 91–101.

Wu, T. T., & Yang, C. N. (1976). Dirac monopole without strings: Monopole harmonics. *Nuclear Physics B, 107*(3), 365–380.

Zhang, Y. H., Tang, C. H., Wen, Q. B., Yang, X. Q., Li, L., & Deng, W. L. (2010). Thermal aggregation and gelation of kidney bean (*Phaseolus vulgaris* L.) protein isolate at pH 2.0: Influence of ionic strength. *Food Hydrocolloids, 24*(4), 266–274.

Zhao, J., Tian, Z., & Chen, L. (2011). Effects of deamidation on aggregation and emulsifying properties of barley glutelin. *Food Chemistry, 128*(4), 1029–1036.